SIGNAL TRANSDUCTION

LATS kinase–mediated CTCF phosphorylation and selective loss of genomic binding

Huacheng Luo[1], Qin Yu[1], Yang Liu[1], Ming Tang[1], Mingwei Liang[1], Dingpeng Zhang[1], Tsan Sam Xiao[2], Lizi Wu[3], Ming Tan[4], Yijun Ruan[5], Jörg Bungert[1], Jianrong Lu[1]*

Chromatin topological organization is instrumental in gene transcription. Gene-enhancer interactions are accommodated in the same CTCF-mediated insulated neighborhoods. However, it remains poorly understood whether and how the 3D genome architecture is dynamically restructured by external signals. Here, we report that LATS kinases phosphorylated CTCF in the zinc finger (ZF) linkers and disabled its DNA-binding activity. Cellular stress induced LATS nuclear translocation and CTCF ZF linker phosphorylation, and altered the landscape of CTCF genomic binding partly by dissociating it selectively from a small subset of its genomic binding sites. These sites were highly enriched for the boundaries of chromatin domains containing LATS signaling target genes. The stress-induced CTCF phosphorylation and locus-specific dissociation from DNA were LATS-dependent. Loss of CTCF binding disrupted local chromatin domains and down-regulated genes located within them. The study suggests that external signals may rapidly modulate the 3D genome by affecting CTCF genomic binding through ZF linker phosphorylation.

INTRODUCTION

Metazoan interphase chromosomes are partitioned into discrete megabase-sized topologically associating domains (TADs) that exhibit highly increased contact frequencies within themselves (*1–3*). At higher resolutions, TADs are typically composed of smaller loop structures, referred to as insulated neighborhoods (*4*). The chromatin domain boundaries are strongly enriched for the binding of the architectural protein CCCTC-binding factor (CTCF) (*5, 6*), which is pivotal in organizing chromatin topology by establishing chromatin loops (*7*). The chromatin architectural domains act as insulated units that spatially constrain transcription regulatory circuits (*4, 8*). Interactions between genes and their regulatory elements generally are confined within the same CTCF-mediated loop domains. CTCF-anchored domain boundaries function as barriers to insulate adjacent chromatin domains. Experimental disruption of CTCF binding at loop anchors alters domain insulation and local gene expression (*9–17*). In cancer, somatic mutations occur recurrently at insulated neighborhood boundaries (*11, 13, 18*). DNA hypermethylation occurs at CTCF-binding sites at domain anchors in certain gliomas (*12*). These genetic and epigenetic events perturb CTCF DNA binding, impair the insulation between topological domains, and allow outside enhancers to illegitimately contact and activate otherwise inactive proto-oncogenes located inside the domains (*12, 13*). These studies underscore the functional importance of chromatin topological organization in transcriptional regulation.

While the genome topology is generally stable (*4, 8*), a subset of chromatin architectural domains undergo marked remodeling during the cell differentiation or reprogramming process, which is accompanied by substantial gene expression changes (*19–24*). Moreover, CTCF genomic binding and interphase chromatin topological organization are mostly abolished during mitosis (*25–27*). The molecular mechanisms underlying three-dimensional (3D) genome dynamics during cell differentiation and cell cycle remain to be elucidated. Furthermore, external signals trigger rapid transcriptional responses in cells. Changes in chromatin spatial organization affect gene expression, yet it is largely elusive whether and, if so, how CTCF-mediated 3D genome architecture may reshape in response to outside signals.

The canonical Hippo-LATS signaling pathway is an evolutionarily conserved central regulator of cell proliferation, apoptosis, organ size, tissue homeostasis, and tumorigenesis (*28, 29*). The core to this pathway in mammals is a kinase cascade in which the MST1/2 kinases (orthologs of *Drosophila* Hippo) phosphorylate and activate the LATS1/2 kinases. LATS1/2 kinases are activated by a wide variety of stress signals (*30*). Active LATS1/2 phosphorylate the major downstream effectors, YAP and its paralog TAZ, and prompt their sequestration in the cytoplasm via 14-3-3 binding, leading to apoptosis and growth arrest in cells. In the absence of LATS activation, YAP/TAZ are unphosphorylated and localized in the nucleus, where they associate with the TEA domain (TEAD) family of transcription factors to coactivate a set of genes that promote cell growth and survival. Dysregulation of LATS signaling causes overgrowth and tumorigenesis (*31–33*). YAP/TAZ are pervasively activated in human malignancies and are essential for the initiation or growth of most solid tumors (*29, 34*).

Here, we identified CTCF as a previously unidentified substrate of the LATS kinases. Active LATS directly phosphorylated CTCF in the zinc finger (ZF) linker regions and impaired its DNA binding activity. Genome-wide CTCF DNA binding profiling revealed that LATS-activating cellular stress did not cause widespread loss of CTCF DNA binding in the genome, but rather selectively dissociated it from a small subset of its genomic binding sites, which were enriched for anchors of chromatin domains containing YAP target genes. The stress-induced CTCF phosphorylation and dissociation from DNA were dependent on LATS. Locus-specific loss of CTCF occupancy disrupted local chromatin domains and decreased expression of YAP target genes that were located inside them. Therefore, the study

[1]Department of Biochemistry and Molecular Biology, UF Health Cancer Center, College of Medicine, University of Florida, Gainesville, FL 32610, USA. [2]Department of Pathology, Case Western Reserve University, Cleveland, OH 44106, USA. [3]Department of Molecular Genetics and Microbiology, UF Health Cancer Center, College of Medicine, University of Florida, Gainesville, FL 32610, USA. [4]Center for Cell Death and Metabolism, Mitchell Cancer Institute, University of South Alabama, Mobile, AL 36688, USA. [5]The Jackson Laboratory for Genomic Medicine, Farmington, CT 06030, USA.
*Corresponding author. Email: jrlu@ufl.edu

uncovers signal-responsive plasticity of the 3D genome architecture and identifies CTCF ZF linker phosphorylation as the critical underlying mechanism.

RESULTS

Active LATS kinases phosphorylate CTCF at the ZF linkers

CTCF contains 11 ZFs, and the central ZFs 4 to 7 are responsible for its binding to the core sequence motif that is present in the vast majority of the known CTCF-binding sites (35). For multi-ZF transcription factors, optimal DNA binding requires cooperative binding of adjacent ZFs, and the linkers that connect neighboring ZFs play an important structural role in stabilizing protein-DNA interactions (36). The ZF linkers are often phosphorylated during mitosis, and these events correlate with loss of DNA binding activity and mitotic chromosomal eviction (37–39). Large-scale phospho-proteomic analysis of mitotic cells identified mitosis-preferential phosphorylation events in >1000 proteins, including phosphorylation of human CTCF ZF linkers, in particular threonine (T) 374 (in the linker between ZF4 and ZF5) and serine (S) 402 (in the linker between ZF5 and ZF6) (Fig. 1A) (40). Concurrently, CTCF is excluded from mitotic chromosomes (41). Subsequent global proteomics studies detected phosphorylation of CTCF ZF linkers in asynchronous cells as well (www.phosphosite.org/proteinAction. action?id=1155&showAllSites=true). We reasoned that CTCF ZF linker phosphorylation may also occur in interphase cells and represent a mechanism for signal-responsive inactivation of CTCF DNA binding. However, kinases that mediate CTCF ZF linker phosphorylation and the significance of these phosphorylation events in CTCF-mediated 3D genome organization are not defined.

The phosphorylation sites T374 and S402 in the CTCF ZF linker regions match the consensus phosphorylation motif (HxRxxS/T) for LATS kinases (Fig. 1A) (42, 43). To test whether LATS kinases were able to phosphorylate CTCF, we purified recombinant glutathione S-transferase (GST) fusion proteins that contained wild-type (WT) CTCF ZF linkers or a mutant CTCF, in which T374 and S402 were substituted with glutamate (E). After incubation with active recombinant LATS2 kinase, the WT CTCF protein fragment was phosphorylated at the RxxS/T sites, while T374E/S402E mutant CTCF was not phosphorylated (Fig. 1B), demonstrating that LATS can directly phosphorylate CTCF ZF linkers in vitro.

To examine whether LATS could phosphorylate CTCF in cells, we cotransfected Flag-tagged full-length CTCF into human embryonic kidney (HEK) 293 cells with LATS1 and/or MST2 (fig. S1A), followed by immunoprecipitation with anti-Flag antibodies and immunoblotting for phosphorylation of the RxxS/T sites. LATS activation in transfected cells required the upstream MST kinases (44). Consistently, expression of either LATS1 or MST2 alone caused little phosphorylation of CTCF, but coexpression of both kinases induced strong phosphorylation of CTCF at the RxxS/T sites (Fig. 1C). Mutations at T374 and S402 of CTCF largely abrogated this phosphorylation (Fig. 1C), suggesting that T374 and S402 are the major LATS-mediated phosphorylation sites in CTCF. We developed an antibody specifically recognizing phosphorylated S402 of human CTCF. When probed with this antibody, CTCF was shown to be phosphorylated in cells expressing both LATS1 and MST2 (fig. S1B). Together, the results indicate that activated LATS kinases phosphorylate CTCF primarily at T374 and S402 in cells.

LATS-activating stress signals induce phosphorylation of CTCF ZF linkers

LATS kinases are activated by a wide range of signals, including energy stress, serum starvation, and cell detachment (30). We analyzed whether activation of endogenous LATS kinases may induce CTCF ZF linker phosphorylation. Energy stress such as glucose deprivation reportedly induced LATS activation and YAP phosphorylation (45–47). We stably expressed Flag-tagged CTCF in MCF7 breast cancer cells through lentiviral transduction. When the cells were switched to glucose-free media, YAP S127 (the major LATS phosphorylation site) became phosphorylated (fig. S1C), indicative of LATS activation. Further treatment with 2-deoxy-D-glucose (2-DG), a glucose analog that competitively inhibits glycolysis, caused even more robust YAP S127 phosphorylation (fig. S1D). When Flag-CTCF proteins were immunoprecipitated from the cells under this energy stress, they exhibited increased phosphorylation at the RxxS/T sites (Fig. 1D), although the exact fraction of phosphorylated CTCF remains to be determined.

Serum starvation activated LATS kinases, leading to YAP phosphorylation (48). MCF7 cells stably expressing Flag-CTCF were cultured in serum-free media. LATS kinases were activated, as evidenced by YAP S127 phosphorylation (fig. S1E). We immunoprecipitated Flag-CTCF proteins and found that their phosphorylation at the RxxS/T sites was markedly enhanced in serum-starved cells compared with cells cultured in serum-supplemented media (Fig. 1E).

Cell detachment caused reorganization of cytoskeleton and activation of the LATS kinases (49). Detachment of MCF7 cells stably expressing Flag-CTCF increased CTCF phosphorylation at the RxxS/T sites, including the S402 residue as detected by the phospho-S402–specific antibody (Fig. 1F). Collectively, these results show that LATS-activating signals stimulate CTCF ZF linker phosphorylation.

LATS is required for stress-induced phosphorylation of endogenous CTCF ZF linkers

We further asked whether endogenous CTCF proteins were phosphorylated in response to cellular stress and whether this phosphorylation was LATS dependent. LATS1 and LATS2 share a high degree of homology and functional overlap but exhibit different expression patterns (50). According to transcriptomics analysis (e.g., GSE112295), LATS2 expression is much higher than LATS1 in MCF7 cells. To deplete most of the activity of LATS, we transduced MCF7 cells with lentiviral short hairpin RNA (shRNA) targeting LATS2 (Fig. 1G), followed by glucose starvation or cell detachment. Endogenous CTCF proteins were immunoprecipitated with anti-CTCF antibodies and immunoblotted for phosphorylation at the RxxS/T sites. In empty vector–infected control cells, glucose starvation or cell detachment markedly stimulated endogenous CTCF ZF linker phosphorylation (Fig. 1G). CTCF protein abundance was steady under these conditions (Fig. 1G), implying that phosphorylation may not affect CTCF protein stability. LATS depletion did not affect the basal levels of CTCF phosphorylation in cells under normal conditions but essentially abolished glucose starvation– or cell detachment–induced CTCF ZF linker phosphorylation (Fig. 1G). The results suggest that LATS is required for cellular stress–induced phosphorylation of endogenous CTCF ZF linkers.

LATS translocates into the nucleus in response to glucose starvation

Our study identified CTCF as a previously unknown substrate of the LATS kinases. However, CTCF is a nuclear protein, while LATS
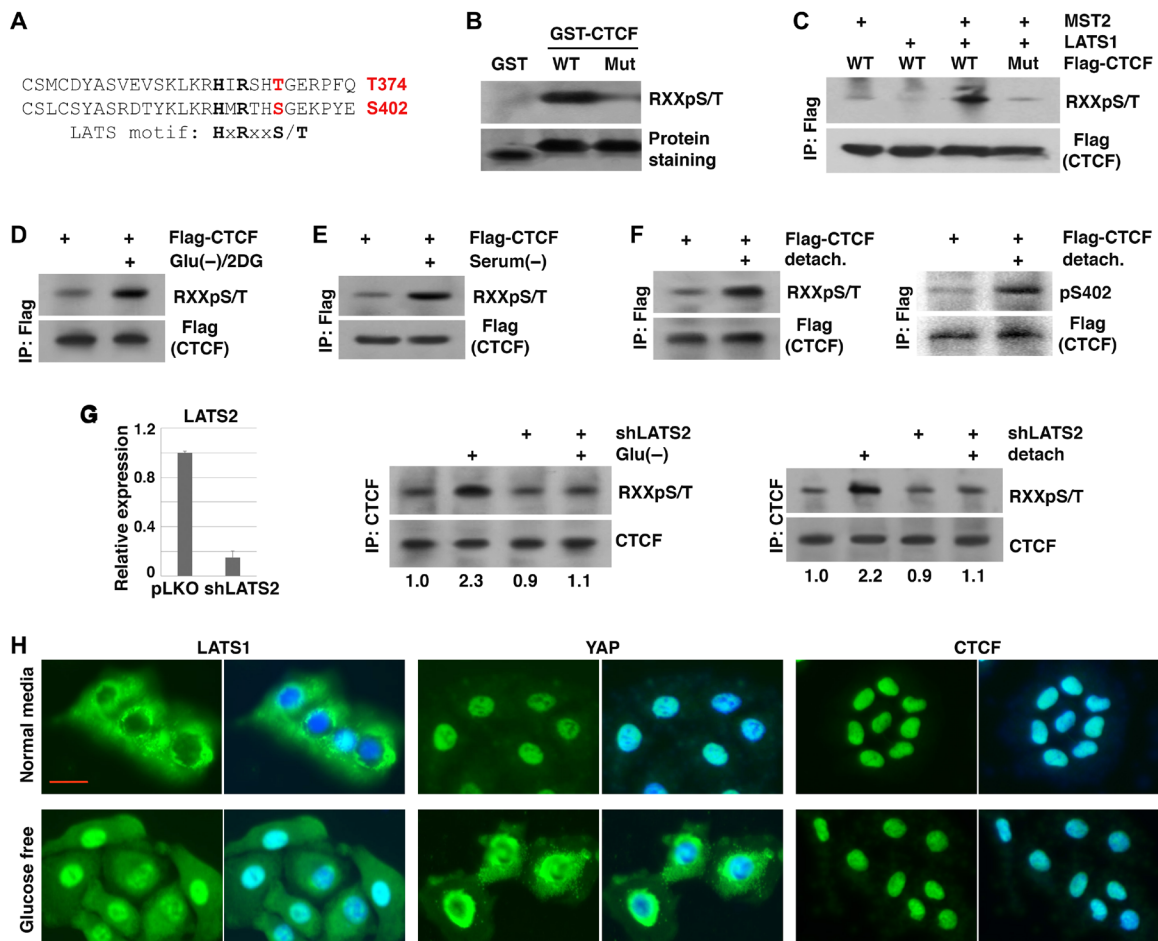
Fig. 1. Phosphorylation of CTCF ZF linkers by stress-activated LATS kinases. (**A**) Phosphorylation sites in CTCF ZF linkers match the LATS kinase phosphorylation motif (HxRxxS/T). (**B**) Direct phosphorylation of CTCF ZF linkers by LATS in vitro. Recombinant glutathione *S*-transferase (GST) and GST-CTCF (amino acids 351 to 410) wild-type (WT) or T374E/S402E mutant (Mut) fusion proteins were incubated with active LATS2 kinase and ATP, followed by immunoblotting with antibodies against phospho-RxxS/T. GST proteins were stained with Coomassie dye. (**C**) LATS kinases induce CTCF ZF linker phosphorylation in cells. Full-length Flag-tagged WT or T374E/S402E Mut CTCF was transfected into HEK293 cells with LATS1 and/or MST2, followed by immunoprecipitation with anti-Flag antibodies and immunoblotting for phosphorylation of RxxS/T. (**D** to **F**) Cellular stress stimulates CTCF ZF linker phosphorylation. MCF7 cells stably expressing Flag-CTCF were cultured in glucose-free [Glu(−)] media supplemented with 2-DG (D), in serum-free [serum(−)] media (E), or in suspension (F) for 1 day. Flag-CTCF proteins were immunoprecipitated with anti-Flag antibodies and immunoblotted for phosphorylation of RxxS/T or S402. (**G**) Energy stress induces endogenous CTCF phosphorylation in a LATS-dependent manner. MCF7 cells were infected with lentiviral vector pLKO or short hairpin RNA (shRNA) targeting LATS2 (shLATS2). The knockdown efficiency was determined by real-time reverse transcription polymerase chain reaction (RT-PCR). Cells were cultured in glucose-free media or in suspension for 1 day and subjected to immunoprecipitation with anti-CTCF antibodies and immunoblotting for phospho-RxxS/T. For quantification, the intensity of phospho-CTCF versus total CTCF in control samples are set at 1.0 (basal levels). The numbers under the blots are fold induction over basal levels. (**H**) LATS nuclear translocation under stress. HCT116 cells were cultured in normal or glucose-free media for 1 day and subjected to immunofluorescence analysis for subcellular localization of indicated proteins. DNA was stained blue with DAPI (4′,6-diamidino-2-phenylindole).

kinases are generally cytoplasmic (*28*, *29*). To investigate where in cells LATS may phosphorylate CTCF, we determined subcellular localization of LATS, YAP, and CTCF in cells under energy stress. We found an antibody against LATS1 that was suitable for immunofluorescence analysis. LATS1 was relatively abundant in HCT116 colon cancer cells (according to the *Cancer Cell Line Encyclopedia*). Under normal culture conditions, LATS1 was detected predominantly in the cytoplasm, whereas YAP and CTCF were exclusively nuclear (Fig. 1H). In cells under glucose starvation, LATS1 was accumulated in the nucleus in the majority of cells, whereas YAP mostly translocated to the cytoplasm, and CTCF remained nuclear (Fig. 1H). It was known that phosphorylation of YAP generated docking sites

for 14-3-3, which promoted YAP cytoplasmic localization (*44*, *51*). In contrast, based on the sequence, phosphorylation of CTCF ZF linkers (T374 and S402) does not create binding sites for 14-3-3. The results suggest that stress-activated LATS moves into the nucleus, where it phosphorylates nuclear substrates YAP and CTCF.

Phosphorylation of the ZF linkers in CTCF impairs its DNA binding activity
Mitotic phosphorylation of ZF linkers correlated with exclusion of ZF proteins from mitotic chromosomes, and phosphomimetic substitutions at ZF linkers abolished DNA binding in vitro (*37*, *38*, *52*, *53*). The crystal structure of the human CTCF DNA binding

domain in complex with DNA was recently solved (*54*). Although neither T374 nor S402 is in direct contact with DNA, phosphorylation of either residue may reduce the overall electrostatic attraction between CTCF and DNA. In addition, both T374 and S402 are adjacent to residues that directly coordinate zinc ions. Their phosphorylation may partially distort the zinc-binding sites, therefore decreasing DNA binding.

We verified whether phosphorylation-mimicking mutations of ZF linker phosphorylation sites (T374 and S402) in CTCF impaired its DNA binding in vitro and in cells. We first purified WT and phosphomimetic mutant CTCF proteins that were transiently expressed in HEK293 cells and incubated them with DNA fragments containing a CTCF-binding site from the *AXL* gene. WT CTCF protein displayed the strongest binding activity, single T374E or S402E mutant showed reduced DNA binding, and the T374E/S402E double mutant exhibited the weakest affinity for DNA (fig. S2A). This observation is consistent with a previous report that phosphorylation of two ZF linkers causes stronger loss of DNA binding activity than phosphorylation of a single linker (*52*). We then stably expressed Flag-tagged WT and phospho-mimetic mutant CTCF in MCF7 cells via lentiviral transduction (fig. S2B), followed by chromatin immunoprecipitation (ChIP) analysis of exogenous CTCF binding at the *AXL* locus with anti-Flag antibodies. Single phosphomimetic mutation at either T374 or S402 substantially decreased CTCF binding, while simultaneous substitutions at both sites maximally reduced CTCF binding (fig. S2B). Therefore, phosphomimetic mutations in CTCF ZF linkers diminish the DNA binding activity of CTCF, implying that ZF linker phosphorylation may disable CTCF from binding to DNA.

Energy stress selectively reduces CTCF occupancy at a small subset of CTCF-binding sites that are most significantly associated with LATS signaling

The impact of external signals on CTCF genomic binding in cells remains poorly understood. LATS kinases phosphorylate CTCF in the ZF linkers and impair its DNA binding activity. However, it was unknown how CTCF occupancy in the genome might be altered by LATS signaling. To address this question, we conducted the CUT&RUN–sequencing (seq) assay (*55*) to map genome-wide CTCF DNA binding in cells under normal versus glucose starvation conditions in two biological replicates (fig. S3A). To facilitate the identification of sites exhibiting differential binding, we used a stringent threshold for peak calling and identified 11,880 CTCF-binding sites in cells in normal media and 11,792 sites in cells in glucose-free media (Fig. 2A). The identified CTCF-bound regions were highly enriched for the known consensus binding motif for CTCF (fig. S3B). Under glucose starvation, CTCF occupancy at most of its genomic targets (10,507) was not altered, but 1363 sites exhibited >2-fold decreased CTCF binding and 1275 sites displayed >2-fold increased CTCF binding (Fig. 2, A and B). Peak annotation, which by default assigns peaks to the nearest transcription start sites (TSS), identified 744 genes that were closest to the 1363 sites showing decreased CTCF binding, and Gene Ontology (GO) pathway analysis revealed that they were most significantly associated with the Hippo-LATS signaling pathway (Fig. 2A and table S1). Sites with increased CTCF binding corresponded to 715 genes, which were most significantly associated with mTOR (mammalian target of rapamycin) signaling (Fig. 2A and table S1). We noticed that representative YAP target genes downstream of LATS signaling (e.g., AMOTL2, AXL, CRY1, GLI2) were all among the 744 genes displaying decreased CTCF binding under glucose starvation

(Fig. 2B). We, thus, analyzed YAP ChIP-sequencing (ChIP-seq) data (GSM2859577) to identify its genomic target genes in MCF7 cells. It turned out that 191 of the 744 genes (25.7%) were potential direct genomic targets of YAP. Together, the results demonstrate that energy stress can rearrange CTCF binding in the genome. In particular, with respect to inactivation of CTCF DNA binding, the LATS-activating signal does not cause global loss of CTCF genomic binding but rather selectively dissociates CTCF from specific subsets of genomic sites that are mostly associated with LATS signaling and highly enrich YAP target genes.

To understand how alterations in CTCF genomic binding were related to gene expression, we analyzed microarray gene expression profiling of MCF7 cells under glucose starvation (*56*). Nearly 600 genes were significantly down-regulated by energy stress (fig. S4A), and they were most significantly associated with the Hippo-LATS signaling pathway (fig. S4B). Representative YAP target genes all displayed reduced expression (fig. S4A). Among the 744 genes that are closest to the genomic sites showing decreased CTCF binding under stress, 293 of them (39%) were down-regulated but very few (3%) were up-regulated (fig. S4C). In addition, 103 of the 191 potential YAP genomic targets were down-regulated. Conversely, among the 715 genes that are closest to sites with increased CTCF binding, 259 (36%) were up-regulated (fig. S4C). Therefore, differential CTCF genomic binding due to energy stress correlates with differential expression of nearby genes. Under energy stress, YAP target genes lose/decrease nearby CTCF binding and concomitantly are down-regulated.

Energy stress preferentially reduces CTCF occupancy at anchors of chromatin loops that contain YAP target genes

CTCF mediates the formation of insulated neighborhoods (*4*). CTCF-anchored chromatin looping interactions in MCF7 cells have been mapped by paired-end tag sequencing (ChIA-PET) analysis (*57*, *58*). To determine how CTCF genomic binding may modulate gene expression, we aligned the differential CTCF-binding sites to CTCF-mediated loop anchors. Among the 1363 sites showing decreased CTCF binding under stress, 821 (60%) were overlapping with loop anchors, and these loops contained 1875 genes. Similarly, 681 of the 1275 sites (53%) with increased CTCF binding also overlapped with loop anchors, and 1657 genes were located in these loops. Among the 597 down-regulated genes under energy stress, 276 were located in chromatin loops whose anchors displayed decreased CTCF binding (198 of them shared the same loop with at least another down-regulated gene), and only 19 were in loops with increased CTCF binding at anchors (fig. S4D). Among the 511 up-regulated genes under energy stress, 225 resided in loops with increased CTCF binding at anchors (162 genes were located in the same loop with at least another up-regulated gene), and 22 were in loops with decreased CTCF binding at anchors (fig. S4D). The results suggest that CTCF-anchored chromatin loops may positively regulate genes inside them.

Because LATS-mediated phosphorylation disrupted CTCF DNA binding and YAP target genes lost CTCF binding under stress, we particularly examined CTCF genomic occupancy at representative YAP target genes. At the *AMOTL2* locus, CTCF-binding peaks generally overlapped with anchors of CTCF-associated chromatin loops, and CTCF occupancy at anchors of a loop domain containing this gene was markedly decreased by glucose starvation (Fig. 2C). Similarly, CTCF binding at the borders of chromatin loops accommodating other YAP target genes (e.g., AXL, BCL2L1, GLI2, LATS2, PFKFB3, TEAD4) also strongly declined in cells under energy stress
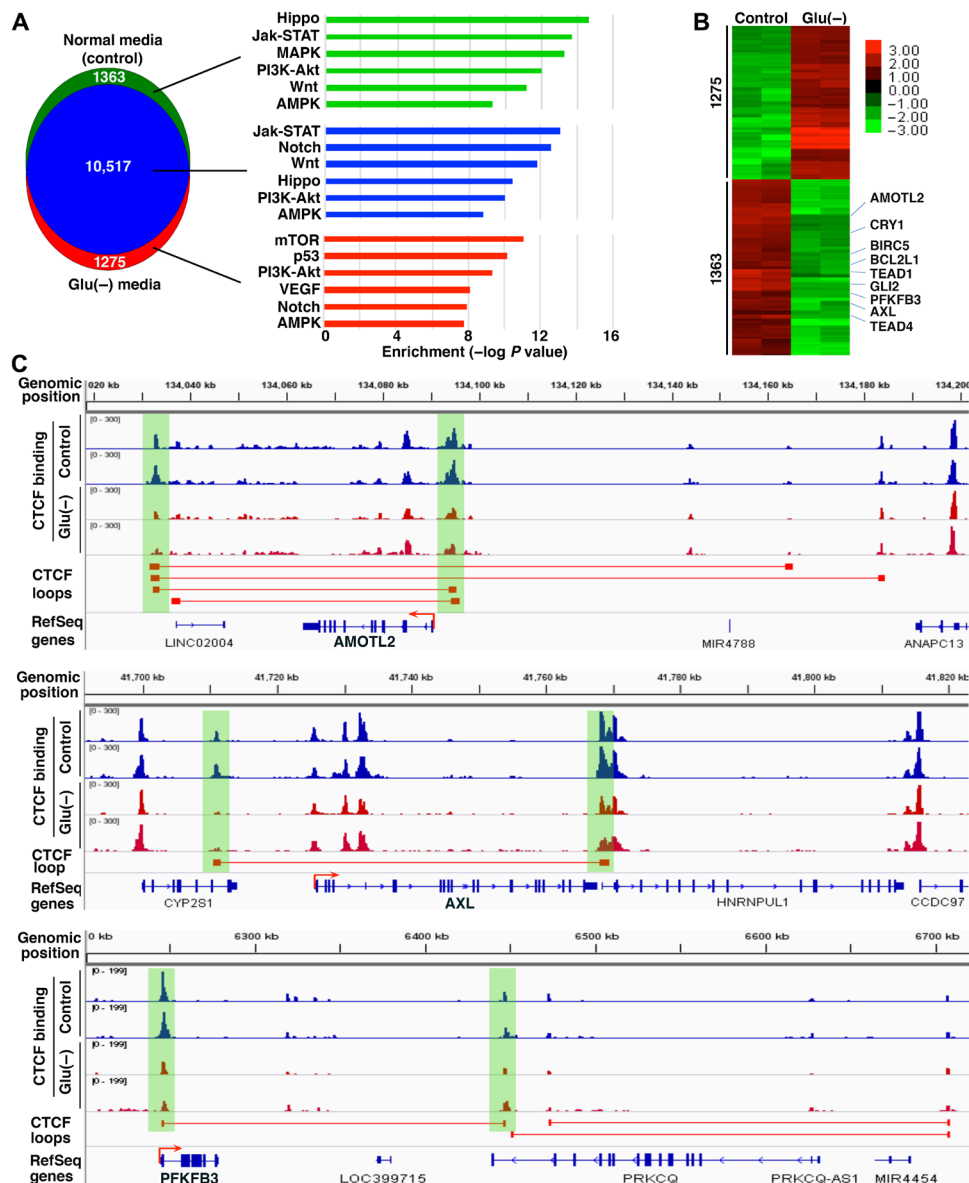
Fig. 2. Energy stress selectively reduces CTCF occupancy at a subset of CTCF-binding sites that anchor chromatin domains enclosing genes associated with LATS signaling. (**A**) Genome-wide mapping of CTCF DNA binding in MCF7 cells in normal (control) and glucose-free [Glu(−)] media. Under glucose starvation, 1363 and 1275 genomic sites show decreased and increased CTCF binding (>2-fold), respectively. Right: GO pathway analysis of genes associated with CTCF-binding sites. AMPK, adenosine monophosphate–activated protein kinase. (**B**) Heatmap of $\log_2$-transformed CTCF-binding signals at genomic sites exhibiting differential binding under glucose starvation [from (A)]. Representative YAP target genes that are closest to the sites with decreased CTCF binding are indicated. (**C**) Glucose starvation specifically reduces CTCF binding at domain boundaries surrounding YAP target genes (*AMOTL2, AXL*, and *PFKFB3*) (highlighted in green), whereas sites outside these chromatin loops are not affected. ChIA-PET interactions of CTCF in MCF7 cells under normal conditions are shown beneath the CTCF genomic binding profiles. The anchors of CTCF loops generally overlap with CTCF-binding peaks. Genomic positions are shown on top.

(Fig. 2C and fig. S5). In notable contrast, CTCF binding in the same genomic regions but outside the chromatin domains containing YAP targets was not affected by glucose starvation (Fig. 2C and fig. S5). The proangiogenic gene vascular endothelial growth factor A (VEGFA) is located in CTCF-anchored chromatin loops (fig. S5). We previously showed that CTCF acts as an enhancer blocker at this locus (*59*). VEGFA is not a YAP target gene, and CTCF binding at loop anchors surrounding VEGFA was insensitive to glucose starvation (fig. S5). The results suggest that LATS-activating energy stress reduces CTCF binding preferentially at the anchors of chromatin domains containing YAP target genes.

We performed standard ChIP assays to validate the loss of CTCF binding at YAP target genes in cells under stress. MCF7 cells were cultured in normal or glucose-free media and subsequently subjected to ChIP analysis of endogenous CTCF with anti-CTCF antibodies. CTCF binding at the anchors of chromatin loops containing representative YAP target genes was substantially decreased by glucose deprivation (Fig. 3A). Expression of YAP target genes was also reduced (fig. S6A). For comparison, CTCF binding at the *VEGFA* locus and VEGFA expression were not altered by energy stress (Fig. 3A and fig. S6A). As cell detachment promoted CTCF ZF linker phosphorylation (Fig. 1),
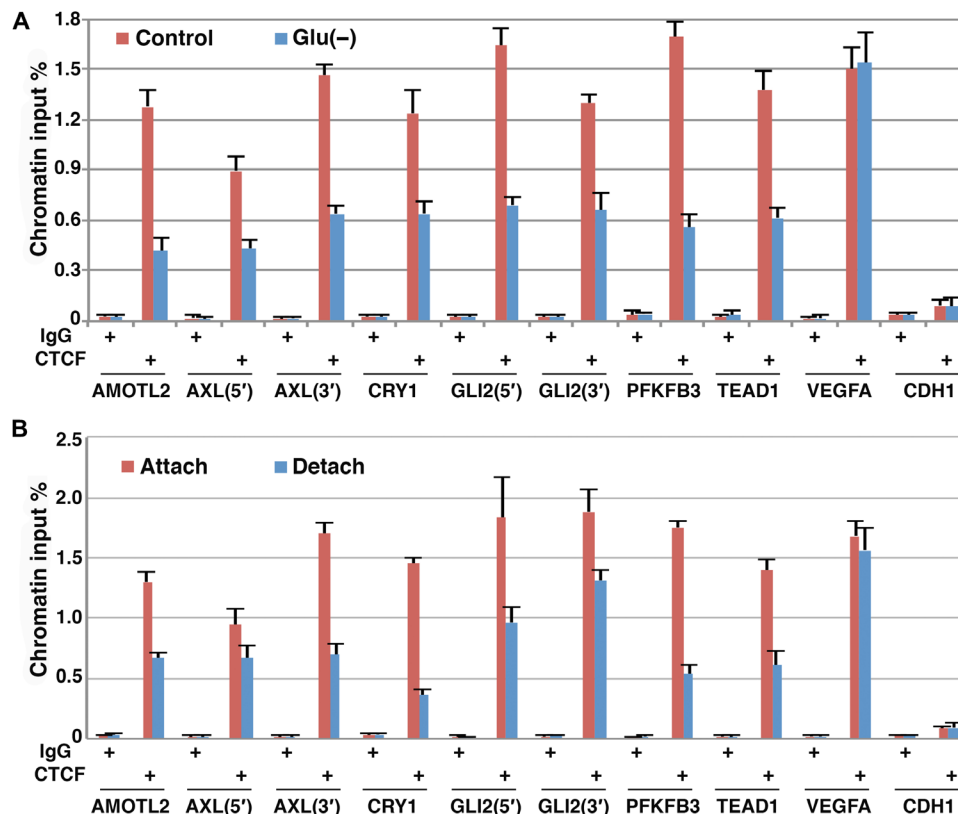
Fig. 3. Cellular stress reduces CTCF binding at chromatin loop anchors surrounding representative YAP target genes. MCF7 cells were cultured in normal or glucose-free media (**A**) or in suspension (**B**) for 1 day, followed by ChIP analysis with anti-CTCF antibodies to determine CTCF binding at the indicated genes. The E-cadherin (CDH1) promoter served as a negative control. Data are represented as mean ± SD. IgG, immunoglobulin G.

CTCF binding at YAP target genes in MCF7 cells was reduced in detached cells, compared with its binding at these loci in attached cells (Fig. 3B). The decrease in CTCF binding was accompanied by reduced expression of YAP target genes (fig. S6B). By contrast, CTCF binding at the *VEGFA* gene or VEGFA expression was not affected by cell detachment (Fig. 3B and fig. S6B). Overall, the results confirm that LATS-activating stress signals impede CTCF binding selectively at YAP target genes and down-regulate their expression.

CTCF binding at insulated neighborhood boundaries may sustain YAP target gene expression

To test whether loss of CTCF DNA binding contributed to down-regulation of YAP targets, we depleted CTCF in MCF7 cells by lentiviral shRNAs (*59*). This led to decreased expression of various YAP target genes (fig. S7A). Similar depletion of CTCF in other cancer cell lines (HCT116 and A549) also down-regulated YAP targets (fig. S7A). The results suggest that CTCF is required to sustain YAP target gene expression.

To unravel how CTCF may support YAP target genes, we examined CTCF DNA binding and chromatin looping at their genomic loci. On the basis of ChIA-PET data, CTCF-binding sites around YAP target genes interacted with each other to form chromosomal loops, and representative YAP target genes along with TEAD/YAP binding peaks are enclosed inside these loops (Fig. 4A). These looping configurations match the pattern of insulated neighborhoods (*4*). Chromatin domains containing YAP target gene AMOTL2, PFKFB3, or BCL2L1 were enriched for the active histone mark

H3 lysine 27 acetylation (H3K27ac) compared with the adjacent regions (Fig. 4A).

PFKFB3 is a key player in tumor metabolism (*60*, *61*). To determine whether CTCF binding at the domain anchors was important for YAP target gene expression, we used CRISPR-Cas9 to introduce small deletions at the CTCF-binding site upstream of the *PFKFB3* promoter in MCF7 cells (Fig. 4B). The YAP/TEAD binding site at the PFKFB3 promoter is downstream of the CTCF site and remained intact in the mutant cells (fig. S7B). ChIP analysis confirmed that ablation of the CTCF site strongly down-regulated CTCF occupancy at the PFKFB3 promoter in two independent mutant clones (Fig. 4C). PFKFB3 expression substantially decreased in the mutant cells (Fig. 4C), suggesting that CTCF binding at the loop anchor is required for PFKFB3 expression. However, because this CTCF site is proximal to the TSS, we cannot exclude the possibility that CTCF may act as a direct transcriptional activator of this gene.

Loss of CTCF binding at YAP target genes due to energy stress is dependent on LATS and YAP

As LATS was required for stress-stimulated CTCF ZF linker phosphorylation (Fig. 1G), we further verified whether loss of CTCF DNA binding at YAP target genes due to energy stress was dependent on LATS. We cultured vector (pLKO)–infected control and LATS2-depleted MCF7 cells in normal or glucose-free media (Fig. 1G) and performed ChIP analysis of CTCF genomic binding at YAP target genes. In normal media, depletion of LATS2 in MCF7 cells did not increase CTCF DNA binding (Fig. 5A and fig. S8), implying that
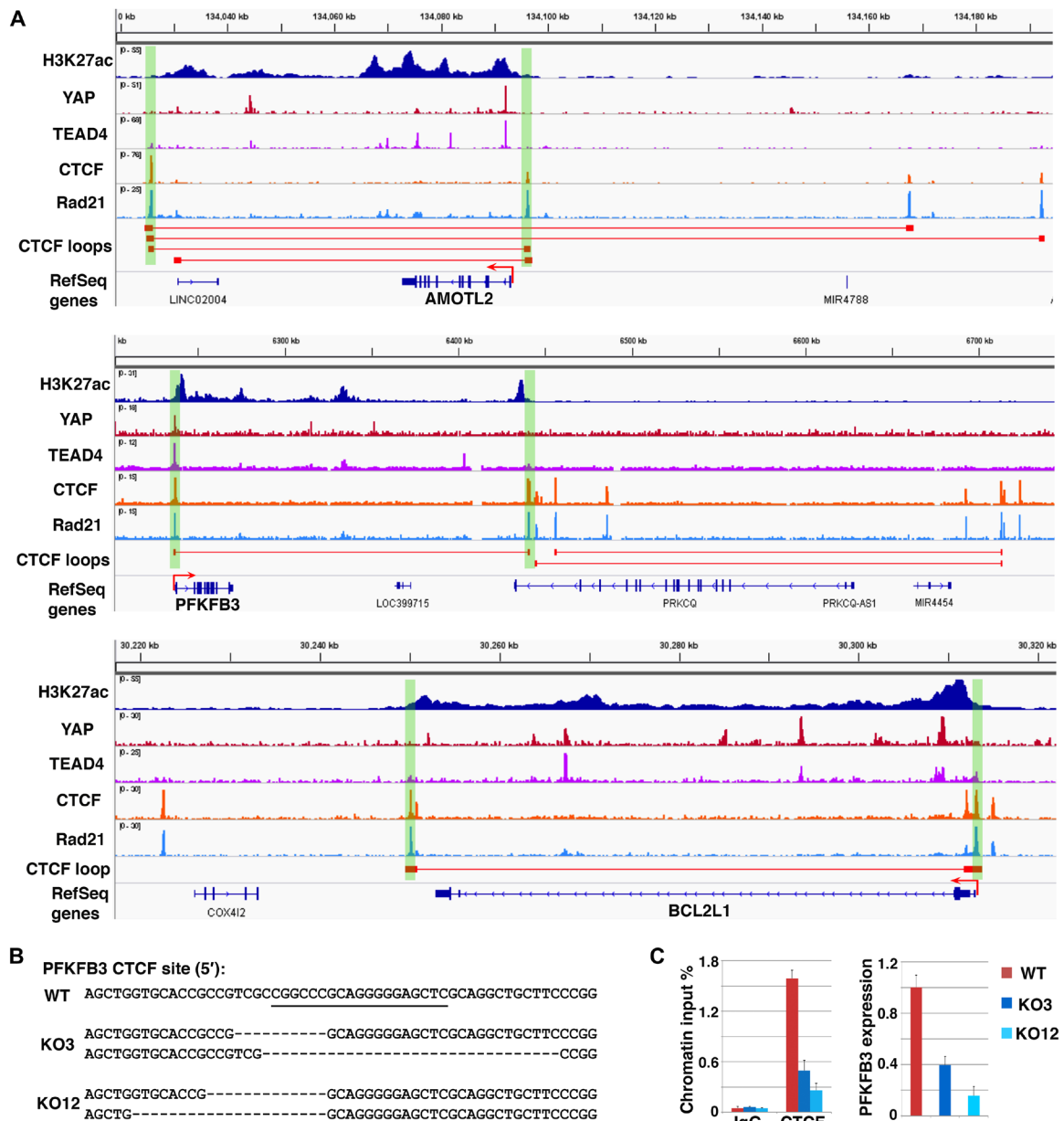
Fig. 4. CTCF-mediated insulated neighborhoods may sustain YAP target gene expression. (**A**) Insulated neighborhoods at the active YAP target gene loci (*AMOTL2*, *PFKFB3*, and *BCL2L1*). CTCF ChIA-PET interactions are displayed below the ChIP-seq profiles of H3K27 acetylation (H3K27ac), YAP, TEAD4, CTCF, and cohesin (Rad21). All epigenomics data except YAP binding (derived from MDA-MB-231 cells) were generated in MCF7 cells. Domain anchors are highlighted in green. (**B**) CRISPR-Cas9–mediated deletion of the CTCF-binding site (underlined) at the *PFKFB3* promoter in two clones (KO3 and KO12) of MCF7 cells. (**C**) CTCF DNA binding is required for PFKFB3 expression. WT, KO3, and KO12 MCF7 cells were subjected to ChIP analysis for CTCF binding at PFKFB3 (left) and to RT-PCR analysis for PFKFB3 expression (right). IgG served as antibody control. Data are represented as mean ± SD.

LATS is essentially inactive under this condition. Glucose starvation substantially reduced CTCF binding at YAP target genes in control cells, but this effect was largely blocked by LATS depletion (Fig. 5A and fig. S8). The result suggests that energy stress–caused dissociation of CTCF from YAP target genes is LATS dependent.

While LATS is required for CTCF ZF linker phosphorylation and loss of DNA binding under stress, it remains elusive how LATS signaling selectively disrupts CTCF DNA binding at specific genomic sites, in particular at the loop anchors surrounding YAP target genes. Because YAP is associated with genomic DNA sites (i.e., primarily TEAD binding sites) inside these chromatin domains, and LATS physically interacts with YAP (*42*, *62*), we postulated that LATS is recruited to these specific genomic regions via interactions with YAP. Although YAP and CTCF generally bind to separate genomic sites due to frequent intradomain chromatin contacts (*4*, *8*), LATS can reach and phosphorylate CTCF that anchors the same domains.

We, thus, examined whether LATS was recruited to YAP/TEAD-binding sites at YAP target genes. We stably expressed Flag-tagged LATS1 in MCF7 cells by lentiviral transduction. Since LATS exhibited dynamic subcellular localization, we examined its potential DNA
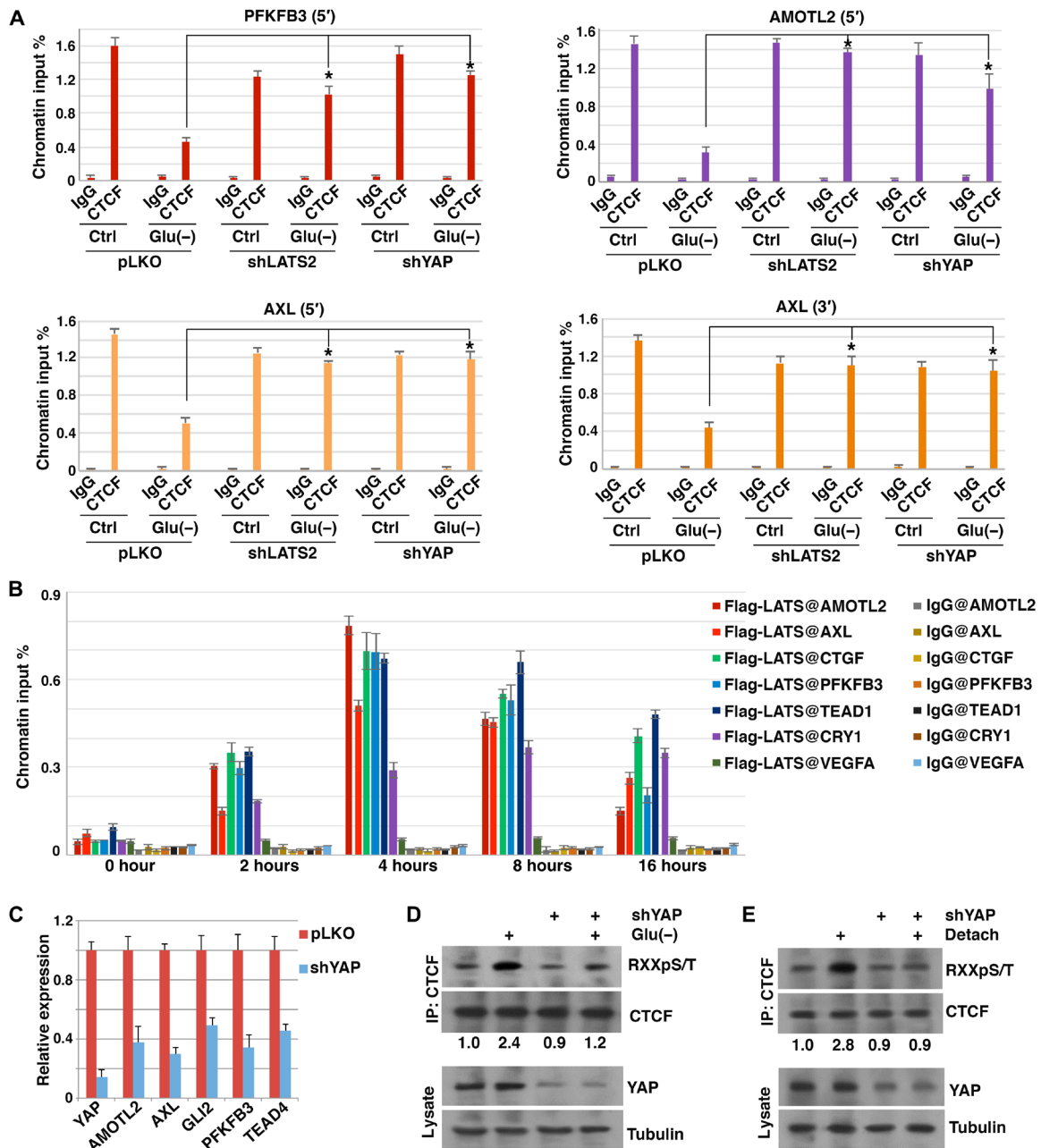
Fig. 5. LATS and YAP are required for stress-induced loss of CTCF DNA binding at YAP target genes. (**A**) Control (pLKO), LATS2-, or YAP-depleted MCF7 cells were cultured in glucose-free media for 1 day, followed by ChIP analysis of CTCF binding at indicated loci. (**B**) LATS is recruited to the YAP/TEAD binding sites under stress. MCF7 cells stably expressing Flag-LATS1 were cultured in glucose-free media at indicated times. Binding of Flag-LATS1 at the YAP/TEAD sites of indicated YAP target genes (VEGFA served as a negative control) was examined by ChIP analysis with anti-Flag antibodies (IgG as antibody control). (**C**) Depletion of YAP in MCF7 cells down-regulates its target genes. MCF7 cells were infected with lentiviral control (pLKO) or shRNA targeting YAP (shYAP). Knockdown efficiency and YAP target gene expression were determined by quantitative RT-PCR. (**D** and **E**) YAP is required for CTCF ZF linker phosphorylation induced by glucose starvation (D) or cell detachment (E). Control and YAP-depleted MCF7 cells were cultured in glucose-free media or in suspension for 1 day. Endogenous CTCF proteins were immunoprecipitated with anti-CTCF antibodies and immunoblotted for RxxS/T phosphorylation. Cell lysates were immunoblotted for YAP. Data are represented as mean ± SD. *$P < 0.05$.

binding at different time points following stress. The cells were starved in glucose-free media for various periods, followed by ChIP analysis with anti-Flag antibodies. Flag-LATS1 was markedly enriched at the YAP/TEAD sites around representative YAP target genes specifically in cells under glucose starvation, with peak binding observed at 4 to 8 hours after starvation (Fig. 5B). The result suggests

that LATS is recruited to genomic sites around YAP target genes under stress.

As YAP may be critical for recruiting LATS, we tested whether YAP deficiency decreased CTCF ZF linker phosphorylation induced by LATS-activating cellular stress. We depleted YAP in MCF7 cells with lentiviral shRNA (Fig. 5C). Depletion of YAP expectedly decreased

its target gene expression (Fig. 5C). Control and YAP-depleted cells were then subjected to glucose starvation or cell detachment, followed by immunoprecipitation of endogenous CTCF and immunoblotting for RxxS/T phosphorylation. YAP depletion largely prevented CTCF ZF linker phosphorylation induced by energy starvation (Fig. 5D) or cell detachment (Fig. 5E). Therefore, YAP critically facilitates stress-induced CTCF ZF linker phosphorylation.

We next investigated whether YAP is required for dissociation of CTCF at YAP target genes under energy stress. Control and YAP-depleted MCF7 cells were cultured in normal or glucose-free media, and subsequently subjected to ChIP analysis of CTCF genomic binding. Depletion of YAP, which reduced YAP target gene expression, had no effect on CTCF DNA binding at YAP target genes in cells cultured in normal media (Fig. 5A and fig. S8). When cells were under glucose starvation, CTCF binding at YAP target genes was diminished in control cells but was largely maintained in YAP-depleted cells (Fig. 5A and fig. S8). Together, these results suggest that YAP is required for LATS-dependent CTCF phosphorylation and loss of DNA binding at YAP target genes.

Cellular stress alters CTCF-mediated insulated neighborhoods

It is poorly understood whether and how CTCF-mediated genome topology may be regulated by external signals. CTCF is absolutely required for 3D genome organization (7). Because cellular stress caused loss of CTCF DNA binding at selected genomic loci such as YAP target genes, we verified whether corresponding 3D chromatin interactions were disrupted. On the basis of ChIA-PET analysis, CTCF anchors a nearly 200-kb chromatin loop spanning the *PFKFB3* locus (Figs. 4A and 6A). We performed quantitative chromosome conformation capture (3C) assays to measure the contact frequency between the loop anchors in MCF7 cells and detected a specific polymerase chain reaction (PCR) product derived from the two interacting CTCF sites (verified by DNA sequencing) (Fig. 6A). As a negative control, a primer from the PFKFB3 3′ untranslated region (3′UTR) failed to generate specific PCR products when combined with the 3C primer from the PFKFB3 5′ region. The result confirmed the specific interaction between the two CTCF-binding sites flanking *PFKFB3*. When MCF7 cells were under glucose starvation, consistent with diminished CTCF binding at this locus, the interaction between these two CTCF sites was substantially decreased (Fig. 6A), demonstrating a loss of CTCF-mediated chromatin looping. By contrast, in the same 3C library samples, CTCF-associated chromatin loop surrounding the *VEGFA* gene (figs. S5 and S9A) was not influenced by glucose starvation (fig. S9B), which is consistent with the persistent CTCF DNA binding at this locus under energy stress (fig. S5).

We also examined the effect of cell detachment on chromatin looping at the *AXL* locus (Figs. 2C and 6B). The 3C analysis validated the existence of a loop structure between the two CTCF-binding sites flanking *AXL*, which were 60 kb apart, in MCF7 cells under normal culture condition (Fig. 6B). This looping conformation was considerably reduced by cell detachment (Fig. 6B). In contrast, the chromatin loop at the *VEGFA* locus was preserved in matrix-detached cells (fig. S9C). Together, cellular stress may selectively disrupt CTCF-anchored chromatin domains encompassing YAP target genes (Fig. 6C).

DISCUSSION
Signal-responsive chromatin topological organization
The vast majority of genes in the genome, along with their regulatory elements, are accommodated in CTCF-organized insulated

neighborhoods (4). This chromatin topological organization represents a fundamental principle underlying mammalian gene transcription (4, 8). However, it is largely elusive whether and how the CTCF-mediated 3D genome architecture may be rapidly remodeled by environmental signals to modulate gene expression. Here, we identified CTCF as a novel substrate of the LATS kinases. LATS can directly phosphorylate CTCF in the ZF linker regions and disable its DNA binding activity. LATS-activating cellular stress causes CTCF phosphorylation and selective dissociation from a subset of genomic sites in a LATS-dependent manner. These genomic sites are most significantly associated with LATS signaling and highly enriched for insulated neighborhood boundaries flanking YAP target genes. Loss of CTCF DNA binding at these sites disrupts corresponding insulated neighborhoods. We, thus, propose the following scenario for cellular stress–induced 3D genome remodeling (Fig. 6C): Under normal culture condition (e.g., with sufficient nutrients), LATS kinases are cytoplasmic and inactive, while YAP is nuclear and binds to its genomic targets. In response to stress signals, LATS kinases are activated and translocate into the nucleus. Through physical interactions with chromatin-associated YAP, LATS kinases are recruited preferentially to insulated neighborhoods containing YAP target genes. Although the CTCF-binding sites and TEAD/YAP-binding sites in the genome are typically separate from each other on linear DNA, due to the high frequency of intradomain chromatin interactions (4, 8), LATS kinases associated with the YAP sites are able to contact and phosphorylate CTCF proteins that anchor the same topological chromatin domains, leading to dissociation of CTCF from DNA and consequent disruption of corresponding insulated neighborhoods. By contrast, insulated neighborhoods that are unable to attract LATS kinases remain unperturbed. Therefore, LATS signaling does not globally block CTCF DNA binding but rather selectively disrupts CTCF occupancy only at a subset of CTCF genomic binding sites, especially the anchors of insulated neighborhoods containing YAP target genes (Fig. 6C). The locus-specific effect specifically affects genes that are concentrated in the LATS signaling pathway. While this model remains to be further validated, external signals may cause certain transcription factors to interfere with CTCF for its DNA binding or DNA hypermethylation at selected CTCF-binding sites, resulting in dissociation of CTCF from DNA. In addition, it is also unclear how some genomic sites gain CTCF binding under stress.

Given the pivotal role of CTCF in chromatin topological organization (7), CTCF ZF linker phosphorylation may represent a general mechanism for inactivation of CTCF and dynamic remodeling of the 3D genome in interphase cells in quick response to external signals. The ZF linkers of CTCF potentially match phosphorylation motifs of various kinases. It is possible that other kinases, when activated by their cognate upstream signals, are recruited to selected genomic loci surrounding their target genes and phosphorylate CTCF proteins that anchor local insulated neighborhoods. This leads to locus-specific loss of CTCF DNA binding and disassembly of chromatin domains, thus eliciting signal-specific transcriptional responses. Overall, the study suggests that interphase genome topological architecture can respond dynamically and rapidly to environmental cues through signal-induced CTCF ZF linker phosphorylation and consequent loss of DNA binding at specific genomic sites. The evolutionarily conserved LATS signaling pathway plays an essential role in mitotic exit (63) and modulates CTCF binding only at a minority subset of genomic sites; therefore, LATS kinases are unlikely to be responsible for CTCF phosphorylation and global exclusion from chromatin during early mitosis.
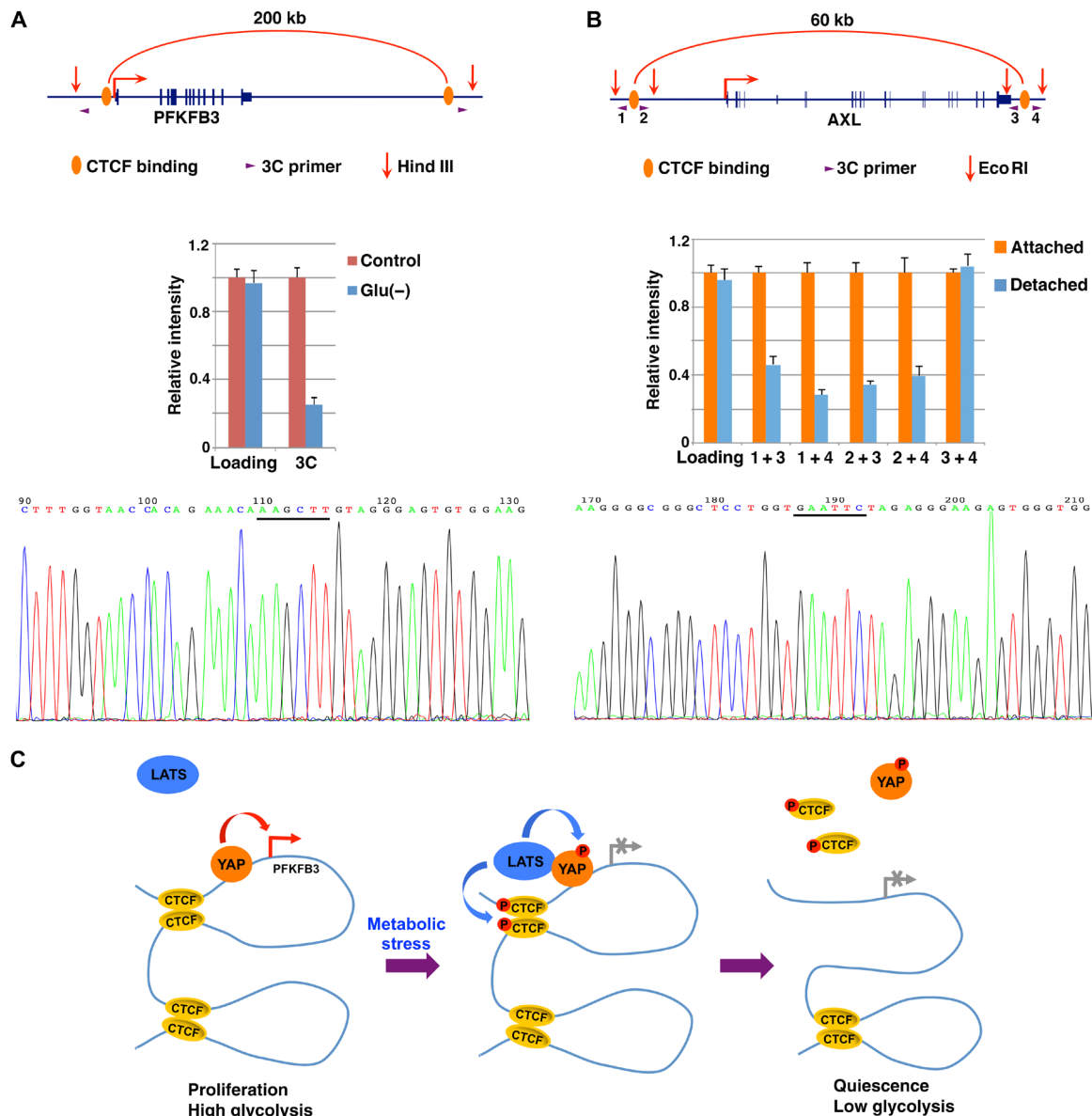
Fig. 6. Cellular stress selectively disrupts CTCF-mediated chromatin loop formation at YAP target genes. (A and **B)** 3C analyses of CTCF-anchored chromatin looping at the *PFKFB3* gene in MCF7 cells under glucose starvation (A) and at the *AXL* gene in MCF7 cells following cell detachment (B). Top: Schematics of CTCF-anchored insulated neighborhoods at the *PFKFB3* (A) and *AXL* (B) loci. Primers and only restriction enzyme sites used in 3C analysis are shown. Middle: Quantitative 3C analysis by real-time PCR. PCR analysis with primers 3 and 4 (for *AXL*) also compares the digestion and ligation efficiencies. Data are represented as mean ± SD. Bottom: Partial sequence of the 3C PCR products shows the junction containing the Hind III site AAGCTT (underlined) (A) or the Eco RI site GAATTC (underlined) from primers 1 and 4 (B). (**C**) LATS kinases selectively disrupt CTCF-mediated insulated neighborhoods. YAP target genes (e.g., *PFKFB3*) are located within CTCF-mediated insulated neighborhoods. Under conditions of high nutrient availability, LATS kinases are inactive, and unphosphorylated YAP binds to its target genes including PFKFB3 (mainly via TEAD) to activate their transcription in the context of insulated neighborhoods. The resulting high PFKFB3 expression expedites glycolysis and cell proliferation. Under energy starvation, LATS kinases are activated, translocate into the nucleus, and physically associate with YAP that is already bound to DNA. Although the YAP binding sites may be distant from the CTCF sites, due to high intradomain interactions, YAP-associated LATS can contact CTCF proteins that anchor the same chromatin domains. Subsequently, LATS kinases phosphorylate YAP and CTCF, dissociating both factors from DNA. Loss of CTCF DNA binding disassembles local insulated neighborhoods. These changes down-regulate YAP target genes including PFKFB3, thereby impeding glycolysis and cell proliferation. For insulated neighborhoods that do not attract LATS (e.g., lacking YAP binding), CTCF DNA binding and chromatin looping remain unaltered under energy stress.

Modulation of insulated neighborhoods

Activation of LATS signaling dissociates CTCF from a subset of genomic sites and reduces expression of local genes. The locus-specific loss of CTCF DNA binding and chromatin looping is unlikely a secondary effect of diminished expression of these genes. In YAP-depleted cells, YAP target genes are down-regulated (Fig. 5C), but CTCF occupancy at the boundaries of chromatin domains containing them is unaltered (Fig. 5A), suggesting that CTCF binding at these sites is independent of YAP or expression of its target genes. Chromatin topological organization is independent of the transcriptional states

of genes located inside the chromatin domains (*64*). By contrast, depletion of CTCF or ablation of CTCF binding decreases YAP target gene expression (Fig. 4 and fig. S7), suggesting that CTCF plays an essential regulatory role in the transcription of the LATS signaling pathway–responsive genes. Together, the results suggest that CTCF-mediated insulated neighborhoods may be required for activation of YAP target genes. Disruption of this domain organization due to loss of CTCF DNA binding may contribute to the down-regulation of YAP targets.

YAP is a transcriptional coactivator and a main effector of LATS signaling. Inactivation of YAP by LATS-mediated phosphorylation is sufficient to down-regulate its target genes. Why does LATS signaling also disrupt CTCF DNA binding and chromatin looping at YAP targets? It is conceivable that CTCF-mediated insulated neighborhoods may provide a conducive epigenetic environment to facilitate YAP-dependent transcriptional activation. Simultaneous loss of both YAP and CTCF not only ensures down-regulation of YAP targets but may also achieve a more durable transcriptional response than inactivation of YAP alone. Therefore, both YAP-associated enhancers and CTCF-mediated chromatin architectural organization may be important for YAP target gene expression. In this regard, in addition to inactivating YAP, LATS kinases may down-regulate downstream target genes, in part, through CTCF phosphorylation and consequent 3D genome architectural remodeling.

MATERIALS AND METHODS
Cell culture, chemical reagents, and antibodies
The HEK293, MCF7 breast cancer cells, and A549 lung cancer cells were cultured in Dulbecco's modified Eagle's medium (DMEM) supplemented with 10% fetal bovine serum (FBS). HCT116 colon cancer cells were cultured in McCoy's 5A medium with 10% FBS. Cell detachment was achieved by culturing cells in poly–HEMA (2-hydroxyethyl methacrylate)–coated dishes. Where indicated, the following drugs were used: phosphatase inhibitors (10 mM sodium fluoride, 10 mM sodium pyrophosphate) and 2-DG (25 mM) were from Sigma. Glucose-free DMEM was from Thermo Fisher Scientific. The following antibodies were obtained commercially: anti-CTCF (Cell Signaling Technology, #3418), anti–phospho-RxxS/T motif (Cell Signaling Technology, #9614), anti-LATS1 (Cell Signaling Technology, #3477), anti-MST2 (Cell Signaling Technology, #3952), anti-YAP (Cell Signaling Technology, #14074), anti–phospho-YAP (S127) (Cell Signaling Technology, #13008), anti-Flag (Sigma, #F1804), and anti-tubulin (Sigma, #T9026). Rabbit polyclonal anti–phospho-CTCF (S402) antibodies were custom generated using a specific phospho-peptide (GenScript).

Plasmids, shRNA-mediated knockdown, and reverse transcription quantitative PCR
Lentiviral shRNAs targeting human CTCF, LATS1, LATS2, YAP, and PFKFB3 were obtained from the pLKO.1-based TRC (The RNAi consortium) library (Addgene, #10878). Cells were infected with lentivirus and followed by puromycin selection. For reverse transcription PCR (RT-PCR), cells were lysed in TRIzol reagent (Invitrogen, #15596026), followed by total RNA purification. Reverse transcription of RNA was conducted using Moloney murine leukemia virus reverse transcriptase with random primers. Gene expression was determined by real-time quantitative PCR (qPCR) with the SYBR Green PCR Kit (Applied Biosystems, #4309155). Data were normalized against β-actin.

CRISPR deletion of CTCF-binding site
Guide RNA target sequences were designed using online software TargetFinder (http://crispr.mit.edu/) and cloned into Bsm BI–digested lentiCRISPRv2 (Addgene, 52961) (*65*). Following lentiviral production, MCF7 cells were infected and selected with puromycin. Single clones were picked and genotyped by genomic DNA PCR. PCR products were cloned into the pGEM-T Easy vector (Promega, A1360) and sequenced.

Chromatin immunoprecipitation
The ChIP assay was conducted as previously described (*66*). Briefly, cells were cross-linked with 1% formaldehyde for 10 min. The reaction was stopped by 0.125 M glycine solution. Cross-linked cells were washed in 1× phosphate-buffered saline (PBS) buffer and collected. Cell pellets were washed several times in washing buffer [0.25% Triton X-100, 10 mM EDTA, 0.5 mM EGTA, and 10 mM tris (pH 8.0)] and resuspended in sonication buffer [1 mM EDTA, 0.5 mM EGTA, and 10 mM tris (pH 8.0)], mixed with glass beads, and then subjected to the sonication process. The sonicated samples were diluted with ChIP buffer [0.01% SDS, 1.0% Triton X-100, 1.0 mM EDTA, 20 mM tris (pH 8.0), 150 mM NaCl] and incubated with antibodies against CTCF, YAP, or Flag. The immunoprecipitates were subjected to a series of washing steps to remove nonspecific binding materials. After reverse cross-linking, DNA was purified and then analyzed by real-time qPCR. Final results represent percentage of input chromatin, and error bars indicate SD from triplicate experiments.

Recombinant protein expression, purification
GST fusion proteins CTCF WT and mutant (T374E and S402E) (ZF4-ZF5: amino acids 351 to 410) were generated by PCR, cloned into GST tag bacterial expression vector pGEX-KG, and verified by DNA sequencing and then transformed into BL21 competent cells for protein expression. Protein expression was induced using 0.1 mM isopropyl β-D-1-thiogalactopyranoside and subsequent incubation at 18°C overnight. Protein samples were purified using glutathione-conjugated sepharose and stored at −80°C until use. The homogeneity and concentration of the proteins were estimated by SDS–polyacrylamide gel electrophoresis (PAGE) and Coomassie blue staining with bovine serum albumin (BSA) as a standard control.

In vitro kinase assay
Briefly, the phosphorylation reactions contained 20 mM tris (pH 7.5), 20 mM Hepes (pH 7.5), 5 mM β-glycerophosphate, 1 mM dithiothreitol, 2 mM Na_3VO_4, 100 mM NaCl, 10 mM $MgCl_2$, 0.1 mM adenosine triphosphate (ATP), LATS2 kinase (SignalChem, L02-11G), 100 ng of recombinant GST and GST-CTCF (WT or mutant) purified from bacteria, and were incubated at 30°C for 1 hour. The reaction mixture was separated by SDS-PAGE, and phosphorylated proteins were detected by Western blotting with anti-RXXpS/T antibody.

Protein/DNA binding in vitro, immunoprecipitation, and Western blotting
Flag tagged-CTCF (WT and mutant) proteins from transfected HEK293 cells were obtained by immunoprecipitation with anti-Flag antibodies, followed by elution with Flag peptides. The purified proteins were then incubated with biotin-labeled double-stranded DNA oligos [~70 base pairs (bp)] carrying a CTCF-binding site from the *AXL* gene and then pulled down with reaction buffer [50 mM tris (pH 8.5), 50 mM KCl, 5 mM $MgCl_2$, 0.5% BSA, and 5% glycerol] containing

0.1% NP-40 for 1 hour at 4°C, and then mixed with streptavidin magnetic beads. The beads were washed extensively with the reaction buffer and were analyzed by SDS-PAGE and Western blotting with anti-CTCF antibody. Western blotting followed standard molecular biology procedures. Quantifications of Western blots were performed with ImageJ and reflected the relative amounts as a ratio of phospho-CTCF protein band relative to the lane's loading control.

Chromosome conformation capture assay

A modified 3C assay protocol was conducted as described previously (67, 68). Briefly, 1×10^7 cells were washed in cold PBS buffer. Cells were cross-linked with a final concentration of 2% formaldehyde for 10 min at room temperature, and cross-linking was stopped with glycine (final concentration, 125 mM). Nuclei were collected from the cross-linked cells and then digested with Eco RI or Hind III at 37°C overnight. The restriction enzymes were heat inactivated, and the reaction mixture was diluted in the ligation buffer to favor intramolecular ligation of cross-linked chromatin segments, and the DNA was subjected to ligation with T4 DNA ligase at 16°C for 3 days. The ligation reaction mixtures were incubated overnight at 65°C with the reverse buffer containing proteinase K (final concentrations at 200 µg/ml) to reverse the cross-links and digest the proteins. After the cross-links were reversed, DNA was purified by phenol chloroform extraction and ethanol precipitated. 3C yields a genome-wide ligation product library in which each ligation product corresponds to a specific interaction between the two corresponding loci. The frequency with which a specific 3C ligation product occurs in the library is a measure of the frequency with which the loci are sufficiently close in space to be cross-linked. Real-time PCR amplification with primers across the restriction sites in the specific 3C ligation products was carried out to quantify the frequency with which the loci interact. Loading controls represent total DNA concentrations between 3C library samples (using PCR primers that do not amplify across the restriction sites used during the 3C assays). The PCR products were also analyzed by agarose gel electrophoresis, purified, and verified by DNA sequencing.

CUT&RUN CTCF genomic binding assay

MCF7 cells were cultured in normal or glucose-free media for 24 hours, and 6×10^6 cells were subjected to the CUT&RUN assay with anti-CTCF antibodies (Cell Signaling Technology, 3418) (55). Genomic DNA fragments (200 to 600 bp) were recovered from agarose gels. Library preparation and high-throughput sequencing were conducted by the Genomic Services Laboratory at HudsonAlpha. In replicate experiments, libraries were prepared using Illumina's TruSeq ChIP Sample Preparation Kit (IP-202-1012) according to the manufacturer's instructions. The quality of the library was checked with Agilent TapeStation. Final libraries were subjected to paired-end sequencing of 100-bp length on an Illumina HiSeq 2500 (30 to 40 million reads for each sample). The obtained genome-wide CTCF-binding data were deposited in the National Center for Biotechnology Information, NIH (NCBI) Gene Expression Omnibus (GEO; GSE114319).

Bioinformatic analysis of the ChIP-seq and CUT&RUN datasets

ChIP-seq datasets were obtained from NCBI GEO, using the following GEO Series accession numbers: TEAD4 (GSM1010860), YAP (GSE66081) (69), CTCF (GSM1010734), Rad21 (GSM1010791) (70), and H3K27ac (GSM2483409). CTCF ChIA-PET interactions were from GSM970215

(57, 58). Except YAP binding (derived from MDA-MB-231 cells), all datasets were generated in MCF7 cells. ChIP-seq and CUT&RUN-seq raw reads were trimmed with bbduk.sh (removal of adapters and low-quality reads) (https://jgi.doe.gov/data-and-tools/bbtools/bb-tools-user-guide/bbduk-guide/) and aligned to human genome (hg19) using Bowtie2 (71) with parameters ("-n 1 -m 1 -p 8"), and the quality of the trimmed data was evaluated by FastQC program (www.bioinformatics.babraham.ac.uk/projects/fastqc/). Peaks were identified using the MACS2 program (72) with parameters (high stringent cutoff q value <0.01) and annotated with the command "annotatePeaks.pl" from the HOMER package (73) and GREAT (74). By default, annotatePeaks.pl assigns peaks to the nearest TSS. Genome browser tracks were created with the genomeCoverageBed command in BEDTools (75) and normalized such that each value represents the read count per kilobase pair per million mapped and filtered reads, and data tracks of visualization were normalized to the number of fragments falling within all peaks for each sample (76). BamCoverage was used to generate the bigWig file of fragment or read coverages, and bamCompare was used to compare the difference between these two normalized BAM files (e.g., $\log_2$ratio) based on the number of mapped reads, including control and experimental datasets (76). All sequencing tracks were visualized in the Intergrative Genomics Viewer genome browsers (77). The de novo motif analysis was performed by the "findmotifsgenome.pl" from the HOMER motif discovery algorithm (73). Phyper function (Python) in R package was used to calculate the overlap genes' correlation and significance. Pearson's correlation coefficient and Pearson's χ^2 test were carried out to calculate overall similarity between the replicates of RNA sequencing and ChIP-seq. DEseq2 (Benjamini-Hochberg adjusted $P < 0.1$; FoldChange>2; DEseq method) was also performed to find the differential binding sites between two peak files, including control and experimental (78). Principal components analysis shows clustering differences of the samples using a small number of principal components according to differentially binding sites (79). GO analysis of differentially binding sites (stress experimental condition versus control condition) for CTCF CUT&RUN-seq was carried out with the Database for Annotation, Visualization and Integrated Discovery (DAVID) web tool (https://david.ncifcrf.gov/, Version 6.8) with the adjusted P value $<1 \times 10^{-3}$ (80, 81).

Statistical analyses of experimental data

All statistical analyses were performed using Microsoft Excel. Data are shown in dot plots or histograms as mean ± SD. Statistical analysis between different experimental groups was determined by two-tailed Student's t tests. In general, for samples with low variation, three to five biological replicates per condition were analyzed in each experiment, including RT-qPCR, ChIP-qPCR, and Western blotting. A value of $P < 0.05$ is considered to be statistically significant.

SUPPLEMENTARY MATERIALS

Fig. S1. Activation of LATS induces phosphorylation of CTCF and YAP.
Fig. S2. Phosphorylation-mimicking mutations impair CTCF DNA binding.
Fig. S3. CUT&RUN-seq analysis of CTCF genomic binding under stress.
Fig. S4. Glucose starvation inhibits YAP target gene expression.
Fig. S5. Glucose starvation reduces CTCF binding preferentially at the anchors of CTCF-associated chromatin loops containing YAP target genes (BCL2L1, GLI2, LATS2, and TEAD4).
Fig. S6. Cellular stress down-regulates YAP target genes.
Fig. S7. CTCF is required to sustain YAP target gene expression.
Fig. S8. LATS and YAP are required for energy stress–induced loss of CTCF DNA binding at GLI2.

Fig. S9. Cellular stress does not perturb CTCF-anchored chromatin looping at the *VEGFA* locus.
Table S1. Genomic sites showing decreased CTCF binding under stress.

View/request a protocol for this paper from *Bio-protocol*.

REFERENCES AND NOTES

1. J. R. Dixon, S. Selvaraj, F. Yue, A. Kim, Y. Li, Y. Shen, M. Hu, J. S. Liu, B. Ren, Topological domains in mammalian genomes identified by analysis of chromatin interactions. *Nature* **485**, 376–380 (2012).

2. E. P. Nora, B. R. Lajoie, E. G. Schulz, L. Giorgetti, I. Okamoto, N. Servant, T. Piolot, N. L. van Berkum, J. Meisig, J. Sedat, J. Gribnau, E. Barillot, N. Blüthgen, J. Dekker, E. Heard, Spatial partitioning of the regulatory landscape of the X-inactivation centre. *Nature* **485**, 381–385 (2012).

3. T. Sexton, E. Yaffe, E. Kenigsberg, F. Bantignies, B. Leblanc, M. Hoichman, A. Parrinello, A. Tanay, G. Cavalli, Three-dimensional folding and functional organization principles of the Drosophila genome. *Cell* **148**, 458–472 (2012).

4. D. Hnisz, D. S. Day, R. A. Young, Insulated neighborhoods: Structural and functional units of mammalian gene control. *Cell* **167**, 1188–1200 (2016).

5. R. Ghirlando, G. Felsenfeld, CTCF: Making the right connections. *Genes Dev.* **30**, 881–891 (2016).

6. C. T. Ong, V. G. Corces, CTCF: An architectural protein bridging genome topology and function. *Nat. Rev. Genet.* **15**, 234–246 (2014).

7. E. P. Nora, A. Goloborodko, A. L. Valton, J. H. Gibcus, A. Uebersohn, N. Abdennur, J. Dekker, L. A. Mirny, B. G. Bruneau, Targeted degradation of CTCF decouples local insulation of chromosome domains from genomic compartmentalization. *Cell* **169**, 930–944.e22 (2017).

8. J. R. Dixon, D. U. Gorkin, B. Ren, Chromatin domains: The unit of chromosome organization. *Mol. Cell* **62**, 668–680 (2016).

9. J. M. Dowen, Z. P. Fan, D. Hnisz, G. Ren, B. J. Abraham, L. N. Zhang, A. S. Weintraub, J. Schuijers, T. I. Lee, K. Zhao, R. A. Young, Control of cell identity genes occurs in insulated neighborhoods in mammalian chromosomes. *Cell* **159**, 374–387 (2014).

10. V. Narendra, P. P. Rocha, D. An, R. Raviram, J. A. Skok, E. O. Mazzoni, D. Reinberg, CTCF establishes discrete functional chromatin domains at the Hox clusters during differentiation. *Science* **347**, 1017–1021 (2015).

11. X. Ji, D. B. Dadon, B. E. Powell, Z. P. Fan, D. Borges-Rivera, S. Shachar, A. S. Weintraub, D. Hnisz, G. Pegoraro, T. I. Lee, T. Misteli, R. Jaenisch, R. A. Young, 3D chromosome regulatory landscape of human pluripotent cells. *Cell Stem Cell* **18**, 262–275 (2016).

12. W. A. Flavahan, Y. Drier, B. B. Liau, S. M. Gillespie, A. S. Venteicher, A. O. Stemmer-Rachamimov, M. L. Suvà, B. E. Bernstein, Insulator dysfunction and oncogene activation in IDH mutant gliomas. *Nature* **529**, 110–114 (2016).

13. D. Hnisz, A. S. Weintraub, D. S. Day, A. L. Valton, R. O. Bak, C. H. Li, J. Goldmann, B. R. Lajoie, Z. P. Fan, A. S. Sigova, J. Reddy, D. Borges-Rivera, T. I. Lee, R. Jaenisch, M. H. Porteus, J. Dekker, R. A. Young, Activation of proto-oncogenes by disruption of chromosome neighborhoods. *Science* **351**, 1454–1458 (2016).

14. Y. Guo, Q. Xu, D. Canzio, J. Shou, J. Li, D. U. Gorkin, I. Jung, H. Wu, Y. Zhai, Y. Tang, Y. Lu, Y. Wu, Z. Jia, W. Li, M. Q. Zhang, B. Ren, A. R. Krainer, T. Maniatis, Q. Wu, CRISPR inversion of CTCF sites alters genome topology and enhancer/promoter function. *Cell* **162**, 900–910 (2015).

15. E. de Wit, E. S. Vos, S. J. Holwerda, C. Valdes-Quezada, M. J. Verstegen, H. Teunissen, E. Splinter, P. J. Wijchers, P. H. Krijger, W. de Laat, CTCF binding polarity determines chromatin looping. *Mol. Cell* **60**, 676–684 (2015).

16. A. L. Sanborn, S. S. P. Rao, S. C. Huang, N. C. Durand, M. H. Huntley, A. I. Jewett, I. D. Bochkov, D. Chinnappan, A. Cutkosky, J. Li, K. P. Geeting, A. Gnirke, A. Melnikov, D. McKenna, E. K. Stamenova, E. S. Lander, E. L. Aiden, Chromatin extrusion explains key features of loop and domain formation in wild-type and engineered genomes. *Proc. Natl. Acad. Sci. U.S.A.* **112**, E6456–E6465 (2015).

17. X. S. Liu, H. Wu, X. Ji, Y. Stelzer, X. Wu, S. Czauderna, J. Shu, D. Dadon, R. A. Young, R. Jaenisch, Editing DNA methylation in the mammalian genome. *Cell* **167**, 233–247.e17 (2016).

18. R. Katainen, K. Dave, E. Pitkänen, K. Palin, T. Kivioja, N. Välimäki, A. E. Gylfe, H. Ristolainen, U. A. Hänninen, T. Cajuso, J. Kondelin, T. Tanskanen, J. P. Mecklin, H. Järvinen, L. Renkonen-Sinisalo, A. Lepistö, E. Kaasinen, O. Kilpivaara, S. Tuupanen, M. Enge, J. Taipale, L. A. Aaltonen, CTCF/cohesin-binding sites are frequently mutated in cancer. *Nat. Genet.* **47**, 818–821 (2015).

19. J. R. Dixon, I. Jung, S. Selvaraj, Y. Shen, J. E. Antosiewicz-Bourget, A. Y. Lee, Z. Ye, A. Kim, N. Rajagopal, W. Xie, Y. Diao, J. Liang, H. Zhao, V. V. Lobanenkov, J. R. Ecker, J. A. Thomson, B. Ren, Chromatin architecture reorganization during stem cell differentiation. *Nature* **518**, 331–336 (2015).

20. P. H. Krijger, B. Di Stefano, E. de Wit, F. Limone, C. van Oevelen, W. de Laat, T. Graf, Cell-of-Origin-Specific 3D genome structure acquired during somatic cell reprogramming. *Cell Stem Cell* **18**, 597–610 (2016).

21. J. A. Beagan, T. G. Gilgenast, J. Kim, Z. Plona, H. K. Norton, G. Hu, S. C. Hsu, E. J. Shields, X. Lyu, E. Apostolou, K. Hochedlinger, V. G. Corces, J. Dekker, J. E. Phillips-Cremins, Local genome topology can exhibit an incompletely rewired 3D-folding state during somatic cell reprogramming. *Cell Stem Cell* **18**, 611–624 (2016).

22. J. E. Phillips-Cremins, M. E. G. Sauria, A. Sanyal, T. I. Gerasimova, B. R. Lajoie, J. S. K. Bell, C. T. Ong, T. A. Hookway, C. Guo, Y. Sun, M. J. Bland, W. Wagstaff, S. Dalton, T. C. McDevitt, R. Sen, J. Dekker, J. Taylor, V. G. Corces, Architectural protein subclasses shape 3D organization of genomes during lineage commitment. *Cell* **153**, 1281–1295 (2013).

23. K. L. Bunting, T. D. Soong, R. Singh, Y. Jiang, W. Béguelin, D. W. Poloway, B. L. Swed, K. Hatzi, W. Reisacher, M. Teater, O. Elemento, A. M. Melnick, Multi-tiered reorganization of the genome during B Cell affinity maturation anchored by a germinal center-specific locus control region. *Immunity* **45**, 497–512 (2016).

24. B. Bonev, N. M. Cohen, Q. Szabo, L. Fritsch, G. L. Papadopoulos, Y. Lubling, X. Xu, X. Lv, J. P. Hugnot, A. Tanay, G. Cavalli, Multiscale 3D genome rewiring during mouse neural development. *Cell* **171**, 557–572.e24 (2017).

25. N. Naumova, M. Imakaev, G. Fudenberg, Y. Zhan, B. R. Lajoie, L. A. Mirny, J. Dekker, Organization of the mitotic chromosome. *Science* **342**, 948–953 (2013).

26. J. H. Gibcus, K. Samejima, A. Goloborodko, I. Samejima, N. Naumova, J. Nuebler, M. T. Kanemaki, L. Xie, J. R. Paulson, W. C. Earnshaw, L. A. Mirny, J. Dekker, A pathway for mitotic chromosome formation. *Science* **359**, eaao6135 (2018).

27. T. Nagano, Y. Lubling, C. Várnai, C. Dudley, W. Leung, Y. Baran, N. Mendelson Cohen, S. Wingett, P. Fraser, A. Tanay, Cell-cycle dynamics of chromosomal organization at single-cell resolution. *Nature* **547**, 61–67 (2017).

28. D. Pan, The hippo signaling pathway in development and cancer. *Dev. Cell* **19**, 491–505 (2010).

29. F. X. Yu, B. Zhao, K. L. Guan, Hippo pathway in organ size control, tissue homeostasis, and cancer. *Cell* **163**, 811–828 (2015).

30. Z. Meng, T. Moroishi, K. L. Guan, Mechanisms of Hippo pathway regulation. *Genes Dev.* **30**, 1–17 (2016).

31. J. Huang, S. Wu, J. Barrera, K. Matthews, D. Pan, The Hippo signaling pathway coordinately regulates cell proliferation and apoptosis by inactivating Yorkie, the Drosophila Homolog of YAP. *Cell* **122**, 421–434 (2005).

32. J. Dong, G. Feldmann, J. Huang, S. Wu, N. Zhang, S. A. Comerford, M. F. Gayyed, R. A. Anders, A. Maitra, D. Pan, Elucidation of a universal size-control mechanism in Drosophila and mammals. *Cell* **130**, 1120–1133 (2007).

33. A. M. Tremblay, E. Missiaglia, G. G. Galli, S. Hettmer, R. Urcia, M. Carrara, R. N. Judson, K. Thway, G. Nadal, J. L. Selfe, G. Murray, R. A. Calogero, C. de Bari, P. S. Zammit, M. Delorenzi, A. J. Wagers, J. Shipley, H. Wackerhage, F. D. Camargo, The Hippo transducer YAP1 transforms activated satellite cells and is a potent effector of embryonal rhabdomyosarcoma formation. *Cancer Cell* **26**, 273–287 (2014).

34. F. Zanconato, M. Cordenonsi, S. Piccolo, YAP/TAZ at the roots of cancer. *Cancer Cell* **29**, 783–803 (2016).

35. H. Nakahashi, K. R. K. Kwon, W. Resch, L. Vian, M. Dose, D. Stavreva, O. Hakim, N. Pruett, S. Nelson, A. Yamane, J. Qian, W. Dubois, S. Welsh, R. D. Phair, B. F. Pugh, V. Lobanenkov, G. L. Hager, R. Casellas, A genome-wide map of CTCF multivalency redefines the CTCF code. *Cell Rep.* **3**, 1678–1689 (2013).

36. S. A. Wolfe, L. Nekludova, C. O. Pabo, DNA recognition by Cys2His2 zinc finger proteins. *Annu. Rev. Biophys. Biomol. Struct.* **29**, 183–212 (2000).

37. S. Dovat, T. Ronni, D. Russell, R. Ferrini, B. S. Cobb, S. T. Smale, A common mechanism for mitotic inactivation of C2H2 zinc finger DNA-binding domains. *Genes Dev.* **16**, 2985–2990 (2002).

38. R. Rizkallah, M. M. Hurt, Regulation of the transcription factor YY1 in mitosis through phosphorylation of its DNA-binding domain. *Mol. Biol. Cell* **20**, 4766–4776 (2009).

39. R. Rizkallah, K. E. Alexander, M. M. Hurt, Global mitotic phosphorylation of C2H2 zinc finger protein linker peptides. *Cell Cycle* **10**, 3327–3336 (2011).

40. N. Dephoure, C. Zhou, J. Villen, S. A. Beausoleil, C. E. Bakalarski, S. J. Elledge, S. P. Gygi, A quantitative atlas of mitotic phosphorylation. *Proc. Natl. Acad. Sci. U.S.A.* **105**, 10762–10767 (2008).

41. K. S. Wendt, K. Yoshida, T. Itoh, M. Bando, B. Koch, E. Schirghuber, S. Tsutsumi, G. Nagae, K. Ishihara, T. Mishiro, K. Yahata, F. Imamoto, H. Aburatani, M. Nakao, N. Imamoto, K. Maeshima, K. Shirahige, J. M. Peters, Cohesin mediates transcriptional insulation by CCCTC-binding factor. *Nature* **451**, 796–801 (2008).

42. Y. Hao, A. Chun, K. Cheung, B. Rashidi, X. Yang, Tumor suppressor LATS1 is a negative regulator of oncogene YAP. *J. Biol. Chem.* **283**, 5496–5509 (2008).

43. B. Zhao, L. Li, K. Tumaneng, C. Y. Wang, K. L. Guan, A coordinated phosphorylation by Lats and CK1 regulates YAP stability through SCF(beta-TRCP). *Genes Dev.* **24**, 72–85 (2010).

44. B. Zhao, X. Wei, W. Li, R. S. Udan, Q. Yang, J. Kim, J. Xie, T. Ikenoue, J. Yu, L. Li, P. Zheng, K. Ye, A. Chinnaiyan, G. Halder, Z. C. Lai, K. L. Guan, Inactivation of YAP oncoprotein by the Hippo pathway is involved in cell contact inhibition and tissue growth control. *Genes Dev.* **21**, 2747–2761 (2007).

45. M. DeRan, J. Yang, C. H. Shen, E. C. Peters, J. Fitamant, P. Chan, M. Hsieh, S. Zhu, J. M. Asara, B. Zheng, N. Bardeesy, J. Liu, X. Wu, Energy stress regulates hippo-YAP signaling involving AMPK-mediated regulation of angiomotin-like 1 protein. *Cell Rep.* **9**, 495–503 (2014).

46. W. Wang, Z. D. Xiao, X. Li, K. E. Aziz, B. Gan, R. L. Johnson, J. Chen, AMPK modulates Hippo pathway activity to regulate energy homeostasis. *Nat. Cell Biol.* **17**, 490–499 (2015).

47. J. S. Mo, Z. Meng, Y. C. Kim, H. W. Park, C. G. Hansen, S. Kim, D. S. Lim, K. L. Guan, Cellular energy stress induces AMPK-mediated regulation of YAP and the Hippo pathway. *Nat. Cell Biol.* **17**, 500–510 (2015).

48. F. X. Yu, B. Zhao, N. Panupinthu, J. L. Jewell, I. Lian, L. H. Wang, J. Zhao, H. Yuan, K. Tumaneng, H. Li, X. D. Fu, G. B. Mills, K. L. Guan, Regulation of the Hippo-YAP pathway by G-protein-coupled receptor signaling. *Cell* **150**, 780–791 (2012).

49. B. Zhao, L. Li, L. Wang, C. Y. Wang, J. Yu, K. L. Guan, Cell detachment activates the Hippo pathway via cytoskeleton reorganization to induce anoikis. *Genes Dev.* **26**, 54–68 (2012).

50. N. Furth, Y. Aylon, The LATS1 and LATS2 tumor suppressors: Beyond the Hippo pathway. *Cell Death Differ.* **24**, 1488–1501 (2017).

51. S. Basu, N. F. Totty, M. S. Irwin, M. Sudol, J. Downward, Akt phosphorylates the Yes-associated protein, YAP, to induce interaction with 14-3-3 and attenuation of p73-mediated apoptosis. *Mol. Cell* **11**, 11–23 (2003).

52. D. Jantz, J. M. Berg, Reduction in DNA-binding affinity of Cys$_2$His$_2$ zinc finger proteins by linker phosphorylation. *Proc. Natl. Acad. Sci. U.S.A.* **101**, 7589–7593 (2004).

53. T. Sekiya, K. Murano, K. Kato, A. Kawaguchi, K. Nagata, Mitotic phosphorylation of CCCTC-binding factor (CTCF) reduces its DNA binding activity. *FEBS Open Bio.* **7**, 397–404 (2017).

54. H. Hashimoto, D. Wang, J. R. Horton, X. Zhang, V. G. Corces, X. Cheng, Structural basis for the versatile and methylation-dependent binding of CTCF to DNA. *Mol. Cell* **63**, 711–720.e3 (2017).

55. P. J. Skene, S. Henikoff, An efficient targeted nuclease strategy for high-resolution mapping of DNA binding sites. *eLife* **6**, (2017).

56. J. L. Chen, D. Merl, C. W. Peterson, J. Wu, P. Y. Liu, H. Yin, D. M. Muoio, D. E. Ayer, M. West, J. T. Chi, Lactic acidosis triggers starvation response with paradoxical induction of TXNIP through MondoA. *PLOS Genet.* **6**, e1001093 (2010).

57. L. Handoko, H. Xu, G. Li, C. Y. Ngan, E. Chew, M. Schnapp, C. W. H. Lee, C. Ye, J. L. H. Ping, F. Mulawadi, E. Wong, J. Sheng, Y. Zhang, T. Poh, C. S. Chan, G. Kunarso, A. Shahab, G. Bourque, V. Cacheux-Rataboul, W. K. Sung, Y. Ruan, C. L. Wei, CTCF-mediated functional chromatin interactome in pluripotent cells. *Nat. Genet.* **43**, 630–638 (2011).

58. Z. Tang, O. J. Luo, X. Li, M. Zheng, J. J. Zhu, P. Szalaj, P. Trzaskoma, A. Magalska, J. Wlodarczyk, B. Ruszczycki, P. Michalski, E. Piecuch, P. Wang, D. Wang, S. Z. Tian, M. Penrad-Mobayed, L. M. Sachs, X. Ruan, C. L. Wei, E. T. Liu, G. M. Wilczynski, D. Plewczynski, G. Li, Y. Ruan, CTCF-mediated human 3D genome architecture reveals chromatin topology for transcription. *Cell* **163**, 1611–1627 (2015).

59. M. Tang, B. Chen, T. Lin, Z. Li, C. Pardo, C. Pampo, J. Chen, C. L. Lien, L. Wu, L. Ai, H. Wang, K. Yao, S. P. Oh, E. Seto, L. E. H. Smith, D. W. Siemann, M. P. Kladde, C. L. Cepko, J. Lu, Restraint of angiogenesis by zinc finger transcription factor CTCF-dependent chromatin insulation. *Proc. Natl. Acad. Sci. U.S.A.* **108**, 15231–15236 (2011).

60. N. Hay, Reprogramming glucose metabolism in cancer: Can it be exploited for cancer. *Nat. Rev. Cancer* **16**, 635–649 (2016).

61. J. Chesney, 6-phosphofructo-2-kinase/fructose-2,6-bisphosphatase and tumor cell glycolysis. *Curr. Opin. Clin. Nutr. Metab. Care* **9**, 535–539 (2006).

62. T. Oka, V. Mazack, M. Sudol, Mst2 and Lats kinases regulate apoptotic function of Yes kinase-associated protein (YAP). *J. Biol. Chem.* **283**, 27534–27546 (2008).

63. A. Hergovich, Hippo signaling in mitosis: An updated view in light of the MEN pathway. *Methods Mol. Biol.* **1505**, 265–277 (2017).

64. C. B. Hug, A. G. Grimaldi, K. Kruse, J. M. Vaquerizas, Chromatin architecture emerges during zygotic genome activation independent of transcription. *Cell* **169**, 216–228.e19 (2017).

65. N. E. Sanjana, O. Shalem, F. Zhang, Improved vectors and genome-wide libraries for CRISPR screening. *Nat. Methods* **11**, 783–784 (2014).

66. H. Luo, A. K. Shenoy, X. Li, Y. Jin, L. Jin, Q. Cai, M. Tang, Y. Liu, H. Chen, D. Reisman, L. Wu, E. Seto, Y. Qiu, Y. Dou, R. A. Casero Jr., J. Lu, MOF acetylates the histone demethylase LSD1 to suppress epithelial-to-mesenchymal transition. *Cell Rep.* **15**, 2665–2678 (2016).

67. J. Dekker, K. Rippe, M. Dekker, N. Kleckner, Capturing chromosome conformation. *Science* **295**, 1306–1311 (2002).

68. X. Li, X. Hu, B. Patel, Z. Zhou, S. Liang, R. Ybarra, Y. Qiu, G. Felsenfeld, J. Bungert, S. Huang, H4R3 methylation facilitates β-globin transcription by regulating histone acetyltransferase binding and H3 acetylation. *Blood* **115**, 2028–2037 (2010).

69. F. Zanconato, M. Forcato, G. Battilana, L. Azzolin, E. Quaranta, B. Bodega, A. Rosato, S. Bicciato, M. Cordenonsi, S. Piccolo, Genome-wide association between YAP/TAZ/TEAD and AP-1 at enhancers drives oncogenic growth. *Nat. Cell Biol.* **17**, 1218–1227 (2015).

70. J. Gertz, D. Savic, K. E. Varley, E. C. Partridge, A. Safi, P. Jain, G. M. Cooper, T. E. Reddy, G. E. Crawford, R. M. Myers, Distinct properties of cell-type-specific and shared transcription factor binding sites. *Mol. Cell* **52**, 25–36 (2013).

71. B. Langmead, C. Trapnell, M. Pop, S. L. Salzberg, Ultrafast and memory-efficient alignment of short DNA sequences to the human genome. *Genome Biol.* **10**, R25 (2009).

72. Y. Zhang, T. Liu, C. A. Meyer, J. Eeckhoute, D. S. Johnson, B. E. Bernstein, C. Nussbaum, R. M. Myers, M. Brown, W. Li, X. S. Liu, Model-based analysis of ChIP-Seq (MACS). *Genome Biol.* **9**, R137 (2008).

73. S. Heinz, C. Benner, N. Spann, E. Bertolino, Y. C. Lin, P. Laslo, J. X. Cheng, C. Murre, H. Singh, C. K. Glass, Simple combinations of lineage-determining transcription factors prime cis-regulatory elements required for macrophage and B cell identities. *Mol. Cell* **38**, 576–589 (2010).

74. C. Y. McLean, D. Bristor, M. Hiller, S. L. Clarke, B. T. Schaar, C. B. Lowe, A. M. Wenger, G. Bejerano, GREAT improves functional interpretation of cis-regulatory regions. *Nat. Biotechnol.* **28**, 495–501 (2010).

75. A. R. Quinlan, I. M. Hall, BEDTools: A flexible suite of utilities for comparing genomic features. *Bioinformatics* **26**, 841–842 (2010).

76. F. Ramirez, F. Dündar, S. Diehl, B. A. Gruning, T. Manke, deepTools: A flexible platform for exploring deep-sequencing data. *Nucleic Acids Res.* **42**, W187–W191 (2014).

77. J. T. Robinson, H. Thorvaldsdóttir, W. Winckler, M. Guttman, E. S. Lander, G. Getz, J. P. Mesirov, Integrative genomics viewer. *Nat. Biotechnol.* **29**, 24–26 (2011).

78. C. S. Ross-Innes, R. Stark, A. E. Teschendorff, K. A. Holmes, H. R. Ali, M. J. Dunning, G. D. Brown, O. Gojis, I. O. Ellis, A. R. Green, S. Ali, S. F. Chin, C. Palmieri, C. Caldas, J. S. Carroll, Differential oestrogen receptor binding is associated with clinical outcome in breast cancer. *Nature* **481**, 389–393 (2012).

79. H. Ji, X. Li, Q. F. Wang, Y. Ning, Differential principal component analysis of ChIP-seq. *Proc. Natl. Acad. Sci. U.S.A.* **110**, 6789–6794 (2013).

80. W. Huang da, B. T. Sherman, R. A. Lempicki, Systematic and integrative analysis of large gene lists using DAVID bioinformatics resources. *Nat. Protoc.* **4**, 44–57 (2009).

81. W. Huang da, B. T. Sherman, R. A. Lempicki, Bioinformatics enrichment tools: Paths toward the comprehensive functional analysis of large gene lists. *Nucleic Acids Res.* **37**, 1–13 (2009).

Citation: H. Luo, Q. Yu, Y. Liu, M. Tang, M. Liang, D. Zhang, T. S. Xiao, L. Wu, M. Tan, Y. Ruan, J. Bungert, J. Lu, LATS kinase–mediated CTCF phosphorylation and selective loss of genomic binding. *Sci. Adv.* **6**, eaaw4651 (2020).